

Modeling and Design of a Micromechanical Phase-Shifting Gate Optical Modulator

Long Que, G. Witjaksono and Y.B. Gianchandani

Department of Electrical and Computer Engineering
University of Wisconsin – Madison, WI, USA, que@cae.wisc.edu

ABSTRACT

This paper reports the modeling and design of a micromechanical optical modulator with a phase-shifting gate that utilizes optical interference effects to modulate light. The gate is opened or closed by microactuators integrated on the same chip, modulating light beams between stationary optical fibers. Modeling results show optimized designs can have high modulation efficiency of 99.5%, and contrast ratio of 23 dB. Alignment between fibers is guaranteed by guiding grooves available in standard MEMS batch fabrication techniques, which also permits coupling distance between fibers to be minimized. The insertion loss for a typical design can be less than -1.9 dB. The beam profile shows negligible distortion for $40\mu\text{m}$ or lower coupling distances.

Keywords: Phase-shifting gate, MEMS, optical interference effects, optical modulation, reflectivity.

1 INTRODUCTION

Low-cost and highly reliable optical devices are needed to implement optical communication networks. Several optical switches have been developed to modulate the optical path using standard microelectromechanical system techniques in the past [1-5]. The most common approach has been to use micromirrors, which present the challenge of high reflectivity and smoothness. The best reflectivity reported to date has been 85% (-0.71dB) by which is achieved by coating gold on a silicon mirror. The roughness of mirror is about 5 nm with proper fabrication process [1].

In this report, a new design of a micromechanical modulator is demonstrated using a phase-shifting gate, which can be driven by microactuators integrated on the same chip. The gate alters the phase of propagated light in the optical system and consequently modulates light by optical interference effects. Modeling efforts show that minimum reflectivity of zero and maximum reflectivity of 99.5% by can be achieved by optimizing the optical systems. The wavelength $\lambda_0 = 1.55 \mu\text{m}$ is used in our

calculations because it is widely used for fiber-optic communication and it is highly transparent and lossless for silicon [6]. Using a phase-shifting gate instead of micromirror simplifies the gate fabrication process [7]: for example, there is no need for a gold evaporation to improve the reflectivity of the gate surface. The coupling distance between fibers can readily be reduced to less than $40 \mu\text{m}$. Fiber alignment is guaranteed by guiding grooves available in standard micromachining process. The scattering of incident light by the gate is negligible since the roughness of the sidewall of the phase-shifting gate can be reduced to several nanometers [1,2,7], while the wavelength for optical communication is generally $1.3 \mu\text{m}$ or $1.55 \mu\text{m}$, which is about 2 orders of magnitude larger than the surface roughness.

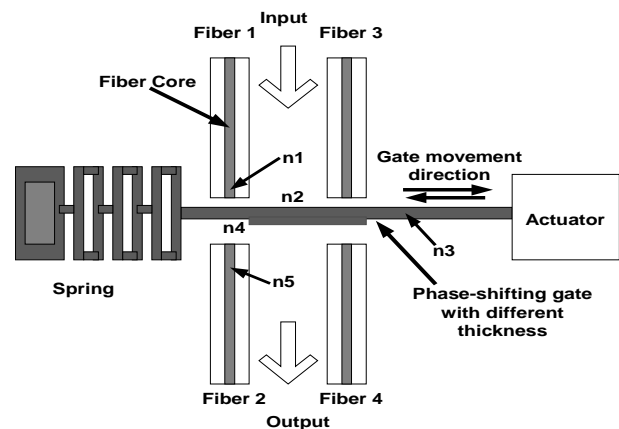


Figure 1: Schematic top view of a typical micromechanical optical modulator

2 DEVICE STRUCTURE

A typical device structure is shown in Figure 1. It consists of a phase-shifting gate with varying thickness. The gate is laterally actuated by integrated electrostatic or an electro-thermal actuators [8,9]. When the gate moves from the right to the left or vice versa, the optical path thickness between fiber 1 and fiber 2 or fiber 3 and fiber 4 will vary, modulating the light due to constructive or destructive optical interference effects.

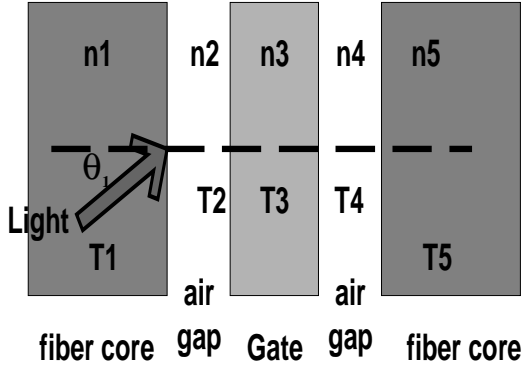


Figure 2: Modeling of the layered structure of the optical modulator system

3 MODELING

The micromechanical optical modulator can be treated as a layered structure optical system for modeling purposes (Figure 2). Here, T_2 and T_4 are the thicknesses of the air gaps, T_3 is the thickness of the phase-shifting gate and $n_1(n_5)$, $n_2(n_4)$, n_3 are the optical refraction indexes of fiber core, air and the gate. Assume the light from fiber is incident at an angle of θ_1 to the air gap layer (Figure 2), so the characteristic matrix of the optical system is given by [10]:

$$M = \begin{pmatrix} \cos \beta_2 & -i/n_2 \sin \beta_2 \\ -in_2 \sin \beta_2 & \cos \beta_2 \end{pmatrix} \times \begin{pmatrix} \cos \beta_3 & -i/n_3 \sin \beta_3 \\ -in_3 \sin \beta_3 & \cos \beta_3 \end{pmatrix} \times \begin{pmatrix} \cos \beta_4 & -i/n_4 \sin \beta_4 \\ -in_4 \sin \beta_4 & \cos \beta_4 \end{pmatrix} \quad (1)$$

and the relative reflectivity of the optical system is given by:

$$R = \frac{\left| (M_{11} + M_{12}P_5)P_1 - (M_{21} + M_{22}P_1) \right|^2}{\left| (M_{11} + M_{12}P_5)P_1 + (M_{21} + M_{22}P_1) \right|^2} \quad (2)$$

where $\beta_i = 2\pi/\lambda_0 n_i T_i \cos \theta_i$ ($i=2,3,4$) and $P_i = n_i \cos \theta_i$ ($i=1,5$), θ_i is the refraction angle in the media with refraction index of n_i ($i=1,2,3,4,5$).

4 OPTIMIZATION

4.1 Structure Dimension Optimization

In the following study assume light wavelength $\lambda_0 = 1.55 \mu\text{m}$ and $\theta_1 = 0$ radian. The design of the system would

be successful if parameters T_2^* , T_3^* and T_4^* could be found for relative reflectivity equal zero or close to unity with a prescribed accuracy:

$$R(T_2^*, T_3^*, T_4^*, \theta_1) = 0 \quad (3)$$

$$\text{or } R(T_2^*, T_3^*, T_4^*, \theta_1) \approx 1 \quad (4)$$

This is a multi-objective optimization problem. A *Matlab*TM program has been developed to solve this problem using *ATTGOAL* routine for the optimization [11]. Like most optimization procedures, this algorithm relies on the starting values of optimization parameters, T_2^0 , T_3^0 and T_4^0 . A proper choice of their values can reduce the computation time. For example, take the starting values to be: $T_2^0 = T_4^0 = 20 \mu\text{m}$, and $T_3^0 = 5 \mu\text{m}$, and the required accuracy as 10^{-4} . For zero reflectivity, the optimized design parameters will be $T_2^* = T_4^* = 20.09 \mu\text{m}$, and $T_3^* = 5.30 \mu\text{m}$, while for maximum reflectivity, the optimized design parameters will be $T_2^* = T_4^* = 19.76 \mu\text{m}$, and $T_3^* = 4.98 \mu\text{m}$.

The algorithm outlined above has applicability for generalized multilayer optics. For the specific example of Figure 2, it provides the intuitively obvious result that the reflectivity is maximum when T_2 and T_4 are odd multiples of $\lambda_0/4n_2$, and T_3 is an odd multiple of $\lambda_0/4n_3$. Additionally, the reflectivity is zero when T_3 is even multiple of $\lambda_0/4n_3$. The analytical formula for these specific conditions can be obtained from equation (1) and (2) as following:

$$R = \left| \frac{i \left(\frac{n_1^2 n_3}{n_2^2} - \frac{n_2^2}{n_3} \right) \sin \beta_3}{-2n_1 \cos \beta_3 + i \left(\frac{n_1^2 n_3}{n_2^2} + \frac{n_2^2}{n_3} \right) \sin \beta_3} \right|^2 \quad (5)$$

The reflectivity versus the gate thickness relationship based on equation (5) is shown in Figure 3. It shows clearly that the light beam can be modulated by the thickness of the gate for the specific dimensional designs.

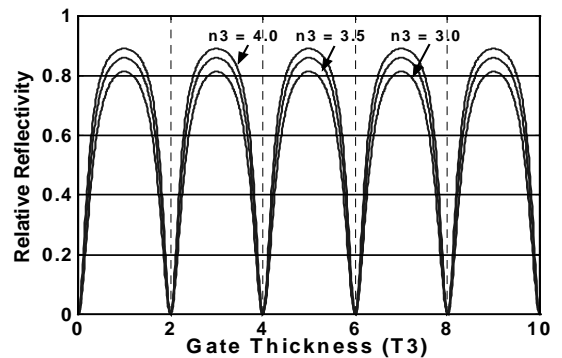


Figure 3: The modulating properties of the layered structure optical system, T_3 in units of $\lambda_0/4n_3$. The modulation efficiency increases with n_3 , $n_1=1.467$, $n_2=1$.

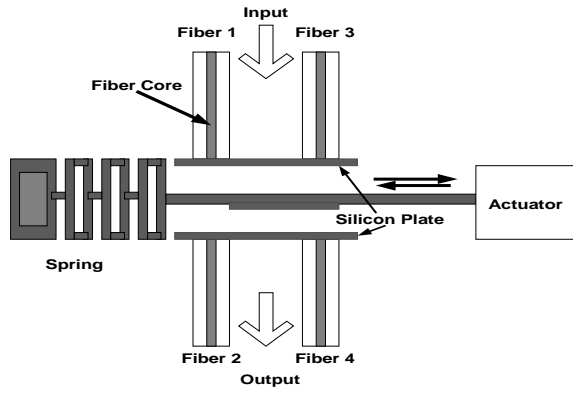


Figure 4: Schematic top view of an optimized design of optical modulator with buffer silicon plates

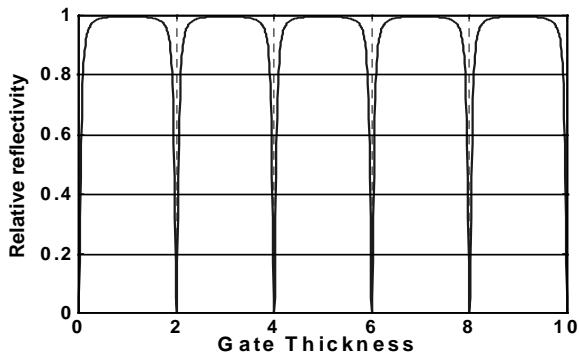


Figure 5: Modulating properties of the layered structure optical system with silicon gates. T_{gate} in units of $\lambda_0/4n_{gate}$.

4.2 System Architecture Optimization

The modulation efficiency can be improved by modifying the system design. Figure 4 shows the buffer silicon plates that are integrated to the optical system to improve the modulation efficiency as well as to assist assembly of the optical fibers. Figure 5 gives the modulation properties of this system with a silicon gate, showing 99.5% modulation and 23 dB contrast ratio can be achieved when the thickness of silicon plates is designed to be odd multiple of $\lambda_0/4n_{silicon}$ and the air gaps are also odd multiple of $\lambda_0/4n_{air}$.

5 DESIGN CONSIDERATION

5.1 Wavelength Dependencies

The effect of quasi-monochromatic light was analyzed for the optical system of Figure 4 at maximum reflectivity, with $T_{plate} = 5.64 \mu\text{m}$, $T_{gate} = 4.98 \mu\text{m}$ and $T_{air} = 19.76 \mu\text{m}$. As shown in Figure 6 even when the light at $\lambda_0 = 1.55 \mu\text{m}$ has a $0.02\mu\text{m}$ distribution, the reflectivity remains almost unchanged. However, beyond this bandwidth, the system shows strong optical filter characteristics.

5.2 Dimensional Error Tolerance

Figure 7 shows the simplified representation of system in Figure 4 which was used to model the dimensional errors. Assume that the modulator is constructed for maximum reflectivity, but the thickness T_{air} has an offset of δT . Under the same design parameters as above (Figure 5), it is found that the reflectivity is a periodic function of δT . Figure 8 shows if the offset is in a range of 0 to $0.3 \mu\text{m}$ or in another period, the variation of relative reflectivity is less than 1%. The small change of reflectivity and its periodic property provide high degree of freedom for design.

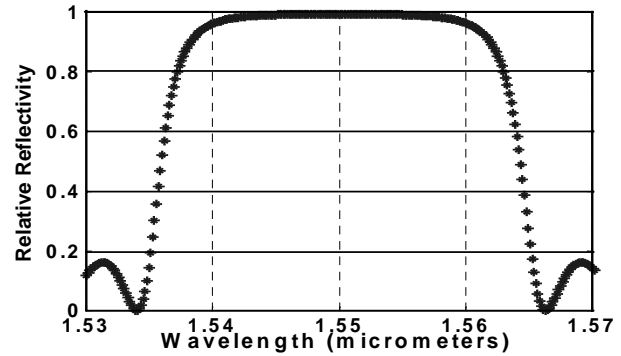


Figure 6: Reflectance wavelength dependencies

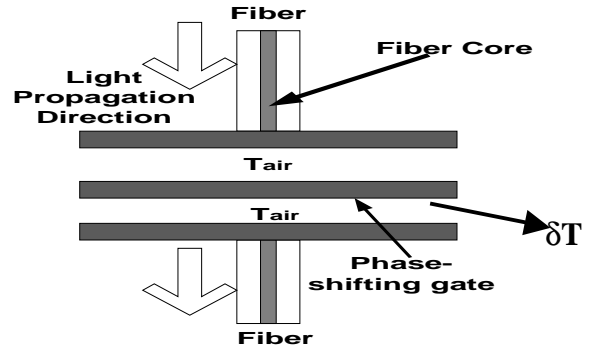


Figure 7: Schematic top view for error analysis with an offset δT of T_{air} for maximum reflectivity situation

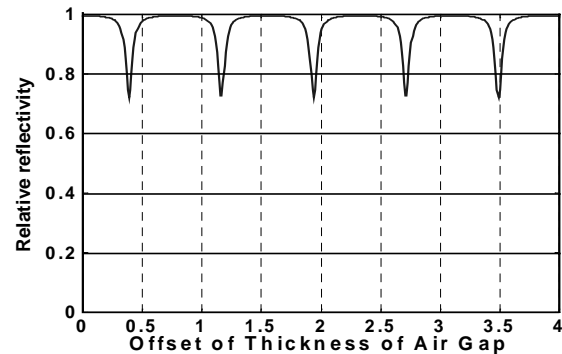


Figure 8: The reflectivity variation due to the offset δT of the target thickness of T_{air}

6 PERFORMANCE ANALYSIS

6.1 Beam Profile after Propagation

The propagation of light in the optical system is modeled using the Beam Propagation Method (BPM) [10] and encoded in *Matlab*. The beam profile emerging from fiber 1 is treated as Gaussian distribution with $\sigma_0 = 5 \mu\text{m}$ for a standard $10 \mu\text{m}$ optical fiber core. Under zero reflectivity conditions, the final beam profiles at the input of fiber 2 for different coupling distances with $n_1=1.467$ (fiber core), $n_2=1.0$ (air), $n_{\text{silicon}}=3.5$ (silicon) are given in Figure 9. If the coupling distance between fibers is less than $40 \mu\text{m}$, the beam profiles have negligible distortion.

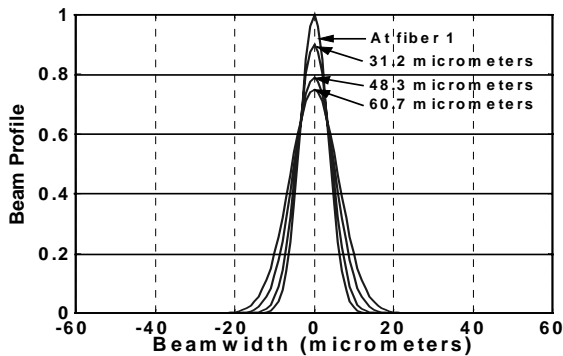


Figure 9: The beam profiles before and after propagation from fiber 1 to fiber 2 with different coupling distance. $T_{\text{gate}}=3.54 \mu\text{m}$ and $T_{\text{plate}}=1.0 \mu\text{m}$ are fixed

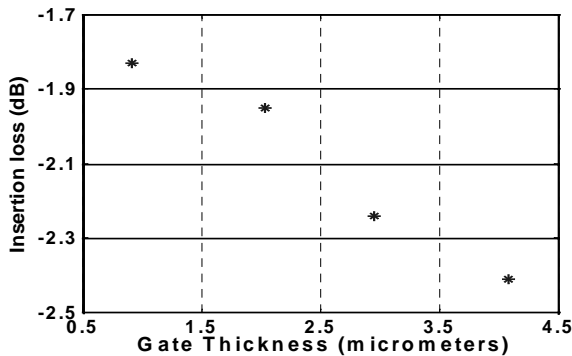


Figure 10: The insertion loss and gate thickness relationship

6.2 Insertion Loss

The insertion loss of the optical system is shown in Figure 10. Assume that the system is in the zero reflectivity condition, the air gaps and the silicon buffer plates are both fixed at odd multiples ($5\lambda_0$ for air gap and $9\lambda_0$ for silicon plate) of $\lambda_0/4n$, and T_{gate} is even multiple of $\lambda_0/4n_{\text{silicon}}$. Evidently, the insertion loss increases with the gate thickness. When the coupling distance reaches $47.47 \mu\text{m}$ and the gate thickness is $2.88 \mu\text{m}$, the insertion loss is about -2.2 dB .

7 CONCLUSIONS

Multi-objective optimization algorithm is demonstrated for the optical design of an optical system with multiple dimensional parameters. Beam propagating profiles and the insertion loss are modeled using Beam Propagation Method. Using these approaches a new micromechanical optical modulator design using phase-shifting gate is proposed and evaluated for the first time. It has a high modulation efficiency of 99.5%, and the insertion loss can be easily kept below -1.9 dB by reducing the coupling distance. The device can be fabricated using standard micromachined techniques. By integrating electrostatic microactuators on the same chip, it is possible that the modulation speed of this device can be upto 100 kHz .

REFERENCES

- [1] W. H. Juan and S. W. Pang, "High aspect ratio Si vertical micromirror array for optical switch", *J. Microelectromech. Syst.*, Vol(17), No.2, 1998, pp 207–213
- [2] Makoto Mita, et al, "Optical and surface characterization of poly-si replica mirrors for an optical fiber switch", *Transducers'99*, pp 332-335
- [3] S. S. Lee, E. Motamedi, and M. C. Wu, "Surface-micromachined free-space fiber optic switches with integrated microactuators for optical fiber communication system", *Transducers'97*, pp 85-88
- [4] R. A. Miller, Y. C. Tai, G. Xu, J. Bartha, and F. Lin, "An electromagnetic MEMS 2×2 fiber optic bypass switch", *Transducers'97*, pp 89-92
- [5] C. Marxer, et al., "Vertical mirrors fabricated by reactive ion etching for fiber optical switch applications," *IEEE Int. Conf. On MEMS'97*, pp 49-54
- [6] D. E. Aspnes, "Optical functions of intrinsic silicon: table of refractive index, extinction coefficient and absorption coefficient vs energy (0 to 400eV)", in *Properties of Silicon*, Emis Data Reviews Series No.4 (IEE, London 1988), Sect. 2.6, pp. 72-79
- [7] Y. Uenish, M. Tsugai and M. Mehregany, "Micro-optomechanical devices fabricated by anisotropic etching of (110) silicon", *J. Micromech. Microeng.*, 1995, pp 305-312
- [8] L. Que, J. Park and Y. Gianchandani, "A bent beam electro-thermal actuator with high force application," *IEEE Int. Conf. On MEMS'99*, pp 31-36
- [9] W.C. Tang, T. U. Chong, H. Nguyen, and R. T. Howe, "Laterally driven polysilicon resonant microstructures," *Sensors and Actuators*, V. 20, 1987, pp.25-32
- [10] Born and Wolf, *Principles of Optics*, 4th edition, Pergamon press, 1970. Pollock, *Fundamentals of Optoelectronics*, R. D. IRWIN, INC., 1995
- [11] *MATLAB 5.3 User's Guide* (1995)